

## ASSESSMENT OF THE TOUGHNESS OF POLYMERS FROM LOW TO HIGH LOADING RATES

H.H. Kausch, Ph. Béguelin

The mode I plane strain fracture toughness at initiation  $K_{Ic}$  of various engineering plastics (PMMA, POM, PEEK) is determined for test speeds between  $10^{-4}$  m/s and 10 m/s, using a high speed servohydraulic testing apparatus. At high rates of testing, the transient acceleration of the specimen is reduced by the use of a damping technique aimed at overcoming dynamic effects.

The  $K_{Ic}$  results obtained are correlated with fractographic analysis performed by SEM and by digital image analysis of macroscopic fracture surfaces. The extent of plastic deformation of POM and PEEK decreases at high rates of deformation which correlates well with the decreasing values of  $K_{Ic}$ . In addition polycarbonate was studied where thin sections of rapidly unloaded crack tips were analyzed by optical microscopy. A multiple crazing mechanism observed at the crack tip at low rates transforms to single craze extension at high rates which decreases  $K_{Ic}$ .

### INTRODUCTION

For scientists, as well as materials manufacturers and design engineers, a knowledge of the behaviour of a given plastic material over a wide range of strain rates and temperatures is of obvious importance. The classical test methods provide either (static) low loading rate material characteristics or impact data. Moreover, even where standard impact tests are employed, interpretation of the data is difficult, and results obtained using static and impact tests cannot be compared.

For strength or toughness studies, fracture mechanics at different loading rates can give useful information on the fracture energy, the deformation, and when existing the toughening mechanisms. The application of fracture mechanics at impact rates is made difficult because of dynamic effects. These mainly result from the high acceleration of the impacted specimen when it comes into contact with the hammer during the early stages of the test. Resonance of both the tested structure and the load sensor often leads to meaningless results.

Department of Materials Science and Engineering, Swiss Federal Institute of Technology, Lausanne, CH-1015 Lausanne

### EXPERIMENTAL METHOD

The method of assessment presented here combines several techniques and overcomes most of these problems [1]. A *servohydraulic* tester provides displacement rates from  $10^{-4}$  to 10 m/s. At high loading rates, the initial transient acceleration of the specimen is considerably reduced by a *damper in the pickup unit* (see fig. 1), leading to stress in equilibrium throughout the specimen, as in static tests. A fibre optical device permits the instantaneous determination of crack opening whereas crack lengths can be followed in real time by the prior application of graphite gauges to the loaded specimen [2].

A conventional force-based analysis has been used to determine the fracture toughness  $K_I$ . The critical stress intensity factor at initiation,  $K_{Ic}$ , has been calculated from the maximum force measured using the damped procedure. The loading situation has been characterized using the crack tip loading rate  $\dot{K}$ . It is calculated from the slope of the force against time,  $\dot{P}$ , measured just before propagation.

$$K_{Ic} = f \frac{P_c}{B\sqrt{W}} \quad \text{and} \quad \frac{dK}{dt} = \dot{K} = f \frac{\dot{P}}{B\sqrt{W}}$$

where  $f$  is a calibration factor dependent on the geometry and crack length,  $P_c$  is the load measured at propagation and  $B$  is the thickness and  $W$  the depth of the specimen.

Considerable information on the nature and extent of deformation of the crack tip plastic zone can be provided by rapid unloading of the specimen, a short time prior to fracture. A technique has been developed to provide specimens unloaded from a well defined stress state for microscopic observations.

This procedure, called the 'twin method', consists of testing simultaneously two specimens placed in series [3]. If the notches are of the same length, one specimen fractures slightly prior the other, unloading its twin quasi-instantaneously. The force being the same for both specimens, the load trace, as well as the displacements measured separately for each specimen, may be used for characterisation. Figure 2 shows the mechanical configuration. Thin sections are then cut from the unfractured specimen and observed by optical microscopy in the unloaded state.

### **EXPERIMENTAL OBSERVATIONS**

Details of the four materials tested are summarized in table I. Specimens have been machined from sheets with  $W = 20$  mm (see figure 2).

	Polymer	Designation	Producer	Manufacturing process	Thickness (B)
PMMA	Poly(methyl-methacrylate)	233	Röhm	Casting	10.1 mm
POM	Polyacetal	Delrin 500	Du Pont	Compression moulding	10.2 mm
PEEK	Polyetheretherketone	450 G	ICI	Injection moulding	~12 mm
PC	Polycarbonate	Makrolon 281	Bayer	Extruded sheets	3 and 10 mm

Table I. Details of the materials used.

#### **PMMA, POM, PEEK**

The tests were conducted at room temperature. PMMA, POM and PEEK were tested at piston velocities from  $10^{-4}$  m/s to 10 m/s. The advantage in plotting the stress intensity factor  $K_{Ic}$  versus the crack tip loading rate is that the only measured variables required are force and time. Thus any change in strain rate at the crack tip between samples having different pre-crack lengths is corrected by the change in compliance.

Figure 3 shows such a plot for the high molecular weight PMMA. Totally or partially stable crack propagation occurred at the lower velocities and is represented by the filled squares in the diagram. At higher opening velocities, the crack propagation was always unstable (open squares). The fracture toughness remained constant over the whole range of crack tip loading rates, as shown by the linear regression analysis (drawn line in figure).

The top scale in this diagram indicates the testing velocity. A similar plot for polyacetal (POM) shows a moderate decrease of the fracture toughness when the loading rate is increased.

The notch sensitivity of PEEK to the loading rate is high, as shown in the same diagram. The drop in fracture toughness with increasing loading rate is considerable, but is found to occur at higher velocities than measured by Karger-Kocsis and Friedrich [4].

#### **Polycarbonate (PC)**

The  $K_{Ic}$  of polycarbonate was measured at room temperature over 5 decades of the testing velocity and the results suggest similar downward trends in the values of  $K_{Ic}$  and  $G_{Ic}$  when the velocity is increased.

The values measured for a sheet of thickness 3 mm are higher than for those of thickness 10 mm. This is explained by the contribution of the deformation in the plane stress region at the free outer surfaces of the sheet, giving rise to an overall initiation value which, according to Williams [5], can be approximated as a linear function of the inverse of the thickness  $B$ . Extrapolation to infinite thickness of the values measured on our two thickness of 3 mm and 10 mm would provide the plane strain values. This has been done for  $K_{Ic}$ , and the result is shown in figure 4.

#### **Crack tip zone analysis on PC specimens**

Thin sections 8 to 10  $\mu\text{m}$  thick have been cut from the central cross-section of specimens unloaded by means of the 'twin method' described earlier. Since both 'twins' had the same initial crack length, these specimens were loaded very close to their critical value of  $K_I$ . Figure 5 shows some microscopical observations in polarized illumination of sections from unfractured twins loaded at  $1 \times 10^{-4}$ ,  $9 \times 10^{-1}$  and  $4.2 \text{ m s}^{-1}$ .

At the lowest testing velocity (fig 5a) the crack has extended by subcritical propagation and several localized deformation zones are visible along the crack and ahead of its tip. Some are also present ahead of the crack tip of twin specimens tested at  $9 \times 10^{-1} \text{ m s}^{-1}$  (fig. 5b). However only a single zone of deformation is observed ahead of the crack tip in the specimens loaded at a velocity of  $4.2 \text{ ms}^{-1}$  (fig. 5c).

Observations by scanning electron microscopy (SEM) of the fracture topology near the crack tip of a 10 mm thick specimen have shown the presence of a process zone located between the pre-crack and the region of unstable crack propagation. In term of its topology this zone can be classified according to three types:

- Type I: subcritical curved-front crack propagation in the centre of the specimen (plane strain region) over a distance less than 1 mm, prior to unstable fracture (see figure 6a).
- Type II: subcritical multiple craze growth in different planes over a distance between 100 and 200  $\mu\text{m}$ . Highly deformed macro-fibrils are drawn from the intersections of these planes (figure 6b).
- Type III: same as type II, but the extension of the craze occurs mainly in a single plane over a distance of 100 to 150  $\mu\text{m}$  (figure 6c).

Note that the fracture surfaces shown in figure 6 are from the fractured twin specimens tested together with those observed in transmitted light in figure 5. It is thus suggested that a process zone with the appearance of that of figure 5a will produce a fracture surface topology of type I, such as shown in figure 6a, and of types II and III for figures 6b and 6c respectively.

## DISCUSSION

In our opinion, the technique used here for high rate testing produces the same severe testing conditions as other undamped impact tests, with three restrictions:

- 1) If one considers the time to fracture as being strictly that elapsed between the first increase of load in the specimen and its fracture, it is from one to three times greater in the damped procedure. One can argue that the decisive mechanisms for fracture occur at high stresses, near the yield stress, and that such high stresses occur in the latter part of the loading step, when the high loading rate has been established.
- 2) In the CT test geometry only one side of the specimen is opened, the other being fixed. At high testing velocity (above  $8 \text{ m s}^{-1}$ ) it has been shown that the time to fracture is too short ( $\sim 0.1 \text{ ms}$ ) to allow quasi-static equilibrium to be reached in the specimen [3]. The stress field is not fully symmetric, and mode II opening occurs at the crack tip. In our case, the ratio of mode II to mode I did not exceed 12 %. Nevertheless, this geometry should not be used in excess of  $10 \text{ m s}^{-1}$ , even with specimens of reduced size such as those used here.
- 3) In a fully dynamic situation (impact), particular stress states such as those resulting from travelling waves or stationary waves can be reached locally. These depend not only on the material but also on the shape and the size of the structure.

## SYMBOLS USED

$K_{Ic}$	=	Stress intensity factor at crack initiation ( $\text{MPa}\sqrt{\text{m}}$ )
CT	=	Compact tension specimen

## REFERENCES

1. Béguelin Ph., Kausch H.H., *The Effect of the Loading Rate on the Fracture Toughness of PMMA, POM, PEEK and mPVC*, to be published in Journal of Materials Science (1994).
2. Stalder B., Béguelin Ph., Roulin-Moloney A.C., Kausch H.H., Journal of Mat. Sci. Vol. 24 (1989) pp. 2262-2274.
3. Béguelin Ph., Kausch H.H., *A Technique for Studying the Fracture of Polymers from Low to High Loading Rates*, European Structural Integrity Society (ESIS) on Impact and Dynamic Fracture of Polymers and Composites, Porto Cervo, Sardinia-Italy, September 20-22. 1993.
4. Karger-Kocsis J., Friedrich K., Polymer Vol. 27 (1986), pp. 1753-1760.
5. Williams J.G., in "Fracture Mechanics of Polymers", Ellis Horwood-Wiley, Chichester (1984).

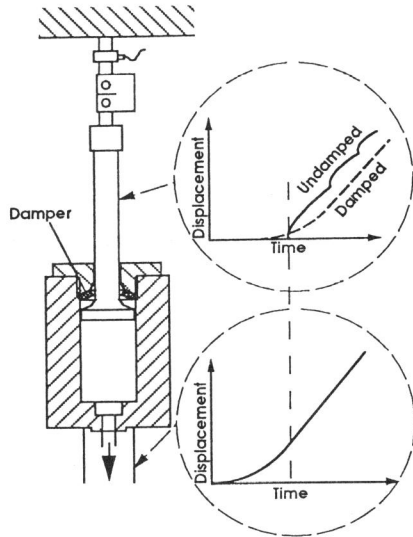


Figure 1. Pick up unit and displacement curves for undamped and damped sample loading.

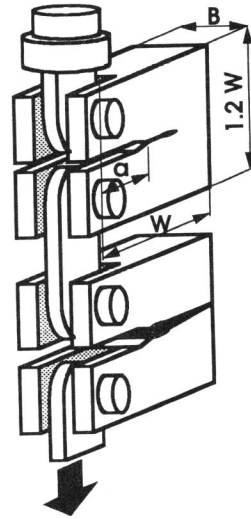


Figure 2. Specimens configuration in the 'twin method'

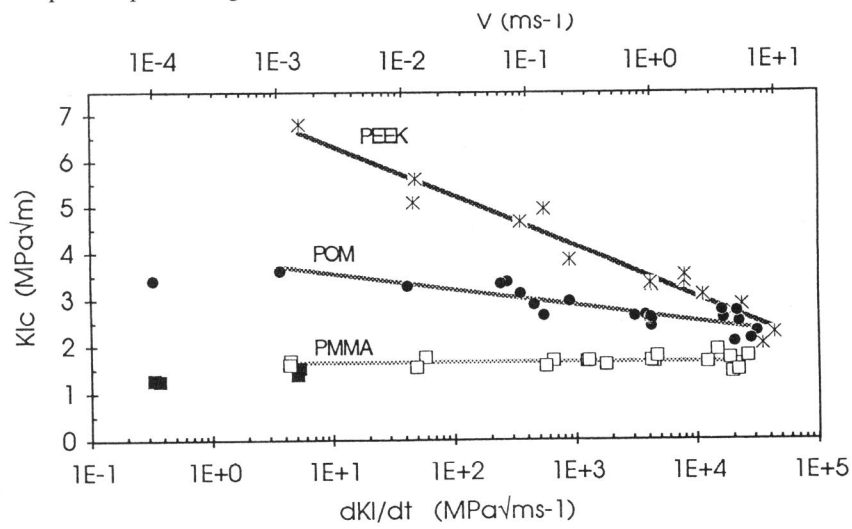


Figure 3. Stress-intensity factor of different polymers as a function of crack tip loading rate.

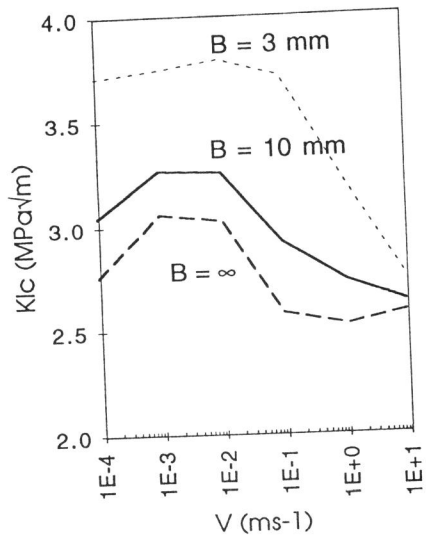


Figure 4.  $K_{Ic}$  versus testing velocity extrapolated for infinite plate thickness

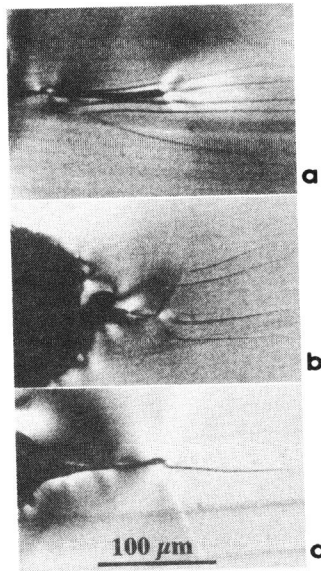


Figure 5. Thin sections of unloaded specimens tested at **a**  $1 \times 10^{-4} \text{ ms}^{-1}$ , **b**  $9 \times 10^{-1} \text{ ms}^{-1}$ , **c**  $4.2 \text{ ms}^{-1}$

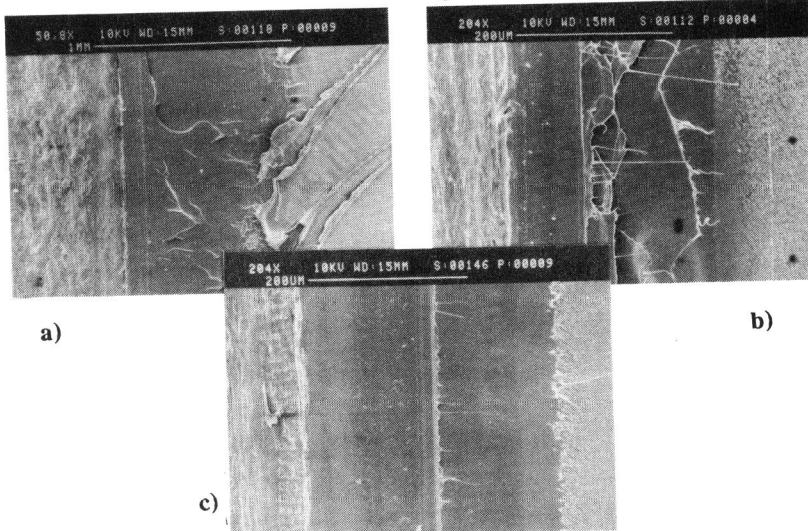


Figure 6. SEM observations near the crack tip. **a** Topology of type I, specimen tested at  $1 \times 10^{-4} \text{ ms}^{-1}$ , **b** Type II,  $9 \times 10^{-1} \text{ ms}^{-1}$ , **c** Type III,  $4.2 \text{ ms}^{-1}$